Carbohydrate Polymers 88 (2012) 690–698

Contents lists available at SciVerse ScienceDirect

Carbohydrate Polymers

journal homepage: www.elsevier.com/locate/carbpol

# Physicochemical properties of high-amylose rice starches during kernel development

Fengling Qin[a], Jianmin Man[a], Canhui Cai[a], Bin Xu[b], Minghong Gu[a,c], Lijia Zhu[a,d], Yong-Cheng Shi[d], Qiaoquan Liu[a,c,*], Cunxu Wei[a,**]

[a] Key Laboratories of Crop Genetics and Physiology of the Jiangsu Province and Plant Functional Genomics of the Ministry of Education, Yangzhou University, Yangzhou 225009, China
[b] Testing Center, Yangzhou University, Yangzhou 225009, China
[c] National Center for Plant Gene Research (Shanghai), Shanghai 200032, China
[d] Department of Grain Science and Industry, Kansas State University, Manhattan, KS 66506, USA

ARTICLE INFO

*Article history:*
Received 7 December 2011
Received in revised form
29 December 2011
Accepted 5 January 2012
Available online 13 January 2012

*Keywords:*
Rice
High-amylose starch granule
Endosperm starch
Kernel development
Physicochemical property

ABSTRACT

In this paper, endosperm starches were isolated from a high-amylose transgenic rice line (TRS) and its wild type rice Teqing (TQ) kernels at different developmental stages. TQ and TRS starches showed similar amylose contents and shapes at early developmental stage, then the amylose content increased with kernel development. The rate of increase in amylose content was much faster in TRS starches than that in TQ starches. TRS starches showed heterogenous granules at the middle and late developmental stages. TQ starch crystallinity remained A-type, but TRS starch crystallinity changed from A- to C- via $C_A$-type. TRS starches showed higher gelatinization temperatures, lower gelatinization enthalpies, lower swelling powers, and lower hydrolysis rates at middle and late developmental stages compared with TQ starches. The amylose content had a significantly negative correlation with crystallinity, gelatinization enthalpy, swelling power, enzyme digestibility, and acid hydrolysis.



## 1. Introduction

Cereal storage starch is a major source of nourishment for humans. Most of the starch in the diets of humans is ingested in cooked foods and digested rapidly in the small intestine. However, a variable proportion is not assimilated in the upper gastrointestinal tract. Instead, this fraction, known as resistant starch (RS), reaches the large intestine where it acts as a substrate for fermentation by the microflora that inhabit that region of the gut (Englyst, Kingman, & Cummings, 1992). Foods high in RS have the potential to improve human health, prevent pathogen infections or diarrhea, and may be of benefit to a variety of pathological processes, such as inflammatory bowel disease, colon cancer risk, insulin resistance and diabetes, and chronic renal or hepatic disease (Nugent, 2005).

Native starch is a mixture of two polysaccharides, linear amylose and highly branched amylopectin, and contains small amounts of non-carbohydrate constituents such as lipid, phosphate and protein. Native starch is stored as discrete semicrystalline granule in plants. In general, RS content of granular starch is positively correlated with the level of amylose (Sang, Bean, Seib, Pedersen, & Shi, 2008). Many high-amylose crop varieties have been developed via mutation or transgenic breeding approaches (Jiang, Campbell, Blanco, & Jane, 2010; Kang, Hwang, Kim, & Choi, 2003; Regina et al., 2006). Some of these starches have been proven to contain a high-level of RS and to show potential health benefits. For example, high amylose wheat grains have a significant potential to improve health by production of increased large-bowel short-chain fatty acids (Regina et al., 2006).

Cereal starch granules with high-amylose content always show markedly different morphology and physicochemical properties compared with waxy and normal starches (Jiang, Campbell et al., 2010; Jiang, Horner et al., 2010; Jiang, Lio, Blanco, Campbell, & Jane, 2010; Kang et al., 2003; Regina et al., 2006). For examples, the normal maize starch granules are spherical and angular, whereas high-amylose *ae* and GENS-0067 mutants consist of about 7% and up to 32% elongated granules, respectively (Jiang, Campbell

*Abbreviations:* AAG, *Aspergillus niger* amyloglucosidase; ATR-FTIR, attenuated total reflectance-Fourier transform infrared; DAF, day after flowering; DSC, differential scanning calorimetry; PPA, porcine pancreatic α-amylase; RS, resistant starch; TQ, Teqing (wild type rice cultivar); TRS, transgenic RS rice line; XRD, X-ray powder diffraction.

* Corresponding author at: Agricultural College, Yangzhou University, Yangzhou 225009, China. Tel.: +86 514 87996648.
** Corresponding author at: College of Bioscience and Biotechnology, Yangzhou University, Yangzhou 225009, China. Tel.: +86 514 87997217.
*E-mail addresses:* qqliu@yzu.edu.cn (Q. Liu), cxwei@yzu.edu.cn (C. Wei).

0144-8617/$ – see front matter © 2012 Elsevier Ltd. All rights reserved.
doi:10.1016/j.carbpol.2012.01.013

et al., 2010). High-amylose wheat starches also display significant morphological alterations (Regina et al., 2006). Normal cereal starches show A-type crystallinity, whereas high-amylose cereal starches have B-type crystallinity (Jiang, Lio et al., 2010; Kang et al., 2003). Compared with normal cereal starches, high-amylose cereal starches have higher gelatinization temperatures, lower gelatinization enthalpies, lower swelling powers, and higher resistances to acid hydrolysis and enzyme digestion (Jiang, Campbell et al., 2010; Kang et al., 2003). The above morphology and physicochemical properties of high-amylose cereal starches are all from mature kernels. Their physicochemical properties during kernel development, however, have been seldom reported in previous research. Recently, Jiang, Horner et al. (2010) and Jiang, Lio et al. (2010) report the formations of elongated starch granules and resistant-starch in high-amylose maize during kernel development. Their results show that many starch granules, each with hilum and growth rings, are initiated in the amyloplast and then fuse. These fused starch granules result in the continuous outer layer, which prevents amyloplast division and forms the elongated starch granules (Jiang, Horner et al., 2010). The increase in the amylose/intermediate component content of the starch during kernel development leads to the formation of long-chain double-helical crystallites that have gelatinization temperatures above 95 °C and result in the increase in the intrinsic RS content of the starch. The increase in the lipid content of the starch can also reduce the enzyme digestibility of the starch (Jiang, Lio et al., 2010).

Rice is the most important cereal crop and the staple food of over half the world's population. Breeding for rice with high amylose and RS contents is of particular interest, as it will be easy to incorporate into the dietary-prevention strategy. A high-amylose transgenic rice line (TRS) has been developed by antisense RNA inhibition of the starch branching enzymes in our laboratory (Wei, Qin, Zhu et al., 2010; Zhu et al., 2011). TRS kernels are rich in RS and have shown significant potential to improve the health of the large bowel in rats (Zhu et al., 2011). Morphological and physicochemical properties of starch granules isolated from TRS mature kernels are markedly different from starches from its wild-type rice Teqing (TQ) mature kernels (Wei, Qin, Zhu et al., 2010; Wei, Xu et al., 2010; Wei et al., 2011). TRS starch is a semicompound starch granule, which consists of many subgranules surrounded by a continuous band, whereas TQ starch is a compound starch granule (Wei, Qin, Zhu et al., 2010). Interestingly, TRS starch is identified as a C-type crystalline starch, which is markedly different from the B-type high-amylose cereal starches (Wei, Xu et al., 2010). TRS starch also has a high resistance to acid hydrolysis, enzyme digestion and heating (Wei, Xu et al., 2010; Wei et al., 2011). The formation of semicompound starch granule in TRS has been observed during kernel development using light microscopy and electron microscopy (Wei, Qin, Zhou et al., 2010). The physicochemical properties of TRS starches during kernel development, however, are not reported.

In this study, endosperm starch granules were isolated from TQ and TRS kernels at different developmental stages. Their crystal properties and thermal properties were investigated by X-ray powder diffraction (XRD), attenuated total reflectance-Fourier transform infrared (ATR-FTIR), and differential scanning calorimeter (DSC). Morphology of starch granule was observed with light microscopy. The amylose contents, swelling powers and hydrolysis properties of developing starches were also determined.

## 2. Materials and methods

### 2.1. Plant material

A transgenic rice line (TRS) with high amylose and RS contents and its wild type rice Teqing (TQ) were used in this study. TRS was generated from the *indica* rice cultivar TQ after transgenic inhibition of two starch branching enzymes (SBEI and SBEIIb) through an antisense RNA technique, and was homozygous for the transgene (Zhu et al., 2011). The expression of SBE I and SBEIIb are completely inhibited in TRS grains (Zhu et al., 2011). The apparent amylose content is dramatically increased from 22.68% to 49.20% in milled rice flour (Wei, Qin, Zhu et al., 2010) and 29.98% to 58.32% in isolated native starch (Wei, Xu et al., 2010), RS content from 1.89% to 14.92% in milled rice flour (Wei, Qin, Zhu et al., 2010). TQ and TRS were cultivated in the transgenic close experiment field of Yangzhou University, Yangzhou, China, in 2010. Individual flowers were tagged at flowering. The kernels were harvested on 3, 5, 7, 10, 13, 16, 20, 25, and 30 day after flowering (DAF) during kernel development and stored at −20 °C.

### 2.2. Isolation of native starch granule

Endosperm was dissected from developing kernels. Native starch granules were isolated from endosperm using the method reported by Wei, Xu et al. (2010).

### 2.3. Morphology of starch granule

Starch granule was examined for the presence of birefringence by using polarized light microscope. A specimen was prepared from the mixture of 2 mg of isolated starch and 1 mL of 50% glycerol solution. The starch granule shape and maltese cross were viewed under the Olympus BX53 polarized light microscope equipped with a CCD camera. Bright field microscope of starch granule was performed as previously described (Wei, Qin, Zhu et al., 2010). The starches were stained with an iodine solution (0.03% $I_2$, 0.09% KI).

### 2.4. Amylose content of starch

Amylose contents of developing starches were determined using the Megazyme Amylose/Amylopectin Assay kit, which is based on the precipitation of amylopectin using concanavalin A. The analysis was performed according to the instructions supplied with the kit. The experiments were performed twice.

### 2.5. XRD analysis

XRD analyses of developing starches were carried out on an XRD (D8, Bruker, Germany), and relative crystallinity (%) of the starches was measured following the method described by Wei, Qin, Zhou et al. (2010). Before measurements, all the specimens were stored in a desiccator where a saturated solution of NaCl maintained a constant humidity atmosphere (relative humidity = 75%) for 1 week.

### 2.6. ATR-FTIR analysis

ATR-FTIR analyses of developing starches were carried out on a Varian 7000 FTIR spectrometer with a DTGS detector equipped with a ATR single reflectance cell containing a germanium crystal (45° incidence-angle) (PIKE Technologies, USA) as previously described (Wei, Xu et al., 2010). The assumed line shape was Lorentzian with a half-width of 19 $cm^{-1}$ and a resolution enhancement factor of 1.9.

### 2.7. Thermal property of starch

Thermal properties of developing starches were analyzed using a DSC (200-F3, NETZSCH, Germany) as described previously (Wei et al., 2011). Starch (5 mg, dry starch basis) was precisely weighed and mixed with 3 times (by weight) deionized-distilled water (15 μL). The mixture was sealed in a aluminum pan overnight at 4 °C. After equilibrating for 1 h at room temperature, the starch

sample was then heated from 25 to 140 °C at a rate of 10 °C/min. The experiments were performed twice.

### 2.8. Swelling power of starch

Swelling powers of developing starches were determined by heating starch–water slurries in a water bath at temperatures of 70 °C and 90 °C according to the procedures of Wei et al. (2011). The experiments were performed in triplicate.

### 2.9. Hydrolysis property of starch

Developing starches were hydrolyzed by porcine pancreatic α-amylase (PPA) (Sigma–Aldrich), *Aspergillus niger* amyloglucosidase (AAG) (Sigma–Aldrich), and HCl. The hydrolysis of starches by PPA and AAG was analyzed using the method of Li, Vasanthan, Hoover, and Rossnage (2004) with some modifications. For PPA hydrolysis, isolated native starch (10 mg) was suspended in 2 mL of enzyme solution (0.1 M phosphate sodium buffer, pH 6.9, 25 mM NaCl, 5 mM $CaCl_2$, 0.02% $NaN_3$, 50 U PPA) and hydrolysis was conducted in a constant temperature shaking water bath with continuous shaking (100 rpm) at 37 °C for 1 day. For AAG hydrolysis, starch (10 mg) was suspended in 2 mL of enzyme solution (0.05 M acetate buffer, pH 4.5, 5 U AAG) and hydrolysis was conducted in a constant temperature shaking water bath with continuous shaking (100 rpm) at 55 °C for 1 day. The hydrolysis of starches by HCl was analyzed using the method of Wei, Xu et al. (2010) with minor modification. 20 mg starch was suspended in 2 mL of 2.2 M HCl and hydrolysis was conducted in a constant temperature shaking water bath with continuous shaking (100 rpm) at 35 °C for 4 days. After hydrolysis, starch slurries were quickly centrifuged (3000 × *g*) at 4 °C for 10 min. The supernatant was used for measurement of the solubilized carbohydrates to quantify the degree of hydrolysis by the anthrone–$H_2SO_4$ method (Viles & Silverman, 1949). The experiments were performed in triplicates.

### 2.10. Correlation analysis

Linear regression and correlation analysis were performed by SPSS 16.0 software. Pearson correlation coefficient and two-tailed test of significance were evaluated to compare the correlation between amylose content and physicochemical properties.

## 3. Results and discussion

### 3.1. Morphology of developing starch granules

Unstained starch granules isolated from mature kernels were observed by polarized light microscope with bright light (Fig. 1A and a). TQ starch granules showed regular and polyhedral shapes with a size of 3–5 μm. The starch granule shapes of TRS were clearly different from those of TQ. Some of the TRS starch granules were large voluminous, non-angular rounded bodies, which were greatly larger than TQ starch granules. Some of the TRS starch granules were elongated, filamentous structures, and some of the granules had similar shapes of TQ starches. Rice starch is a compound starch, which is composed of several separate subgranules or granules. These subgranules come simultaneously in a single amyloplast, but each granule still exhibits a polarizing cross. During starch isolation, the compound starch can be broken up into separate subgranules (Shannon & Garwood, 1984). The large voluminous starch of TRS is a semicompound starch and consists of smaller subgranules, some of which located at the periphery of starch are fused to each other with adjacent ones forming a thick band or wall encircling the entire circumference of starch. The band may prevent the release of subgranules during starch isolation (Wei, Qin, Zhu et al., 2010). The elongated starch granules are also observed in high-amylose maize starches (Jiang, Lio et al., 2010). Under polarized light microscope with polarized light, all TQ starch granules showed birefringence in the form of the typical maltese crosses, indicating a symmetrical radial molecular orientation in the granules (Fig. 1B). The large voluminous and elongated starch granules of TRS showed many maltese crosses, which indicated that these starches consisted of many subgranules (Fig. 1b).

Iodine-stained starches harvested at different kernel developmental stages are shown in Fig. 1. All of TQ starches obtained at different kernel developmental stages had regular and polyhedral shapes (Fig. 1C–L). TQ starch harvested on 3 DAF had smaller granule sizes and was stained more lightly than the starches harvested on later dates. The sizes and staining intensities of these starch granules increased from 3 DAF to 10 DAF. After 10 DAF, TQ starches had similar sizes and staining intensities and were homogeneous. There were no significant differences in shapes and staining intensities between TQ and TRS starches harvested on 3 and 5 DAF (Fig. 1C, D, c and d). Some large voluminous starch granules, which were darkly stained, began to be detected in TRS starches harvested on 7 DAF (Fig. 1e). The elongated starch granules were also detected in TRS starches harvested on 10 DAF (Fig. 1f). After 10 DAF, TRS starches showed clearly heterogeneities and consisted of mainly three types of starch granules, large voluminous, elongated and polyhedral starch granules (Fig. 1g–l). The heterogeneities of TRS starches were also observed in sections of developing endosperm cells under light and electron microscopes (Wei, Qin, Zhou et al., 2010). The elongated and polyhedral starch granules were stained more lightly than the large voluminous starch granules (Fig. 1f–l).

### 3.2. Amylose contents of developing starches

The amylose contents of endosperm starches isolated from TQ and TRS kernels harvested at different developmental stages are shown in Fig. 2. The amylose contents of the TQ starches increased from 3.7% on 3 DAF to 14.5% on 10 DAF, 18.0% on 20 DAF and 18.7% on 30 DAF (Fig. 2). This result indicated that the amylose contents in TQ increased during the developmental stage, with the fast increase before 10 DAF and slow increase from 10 DAF to 20 DAF, and remained a similar level after 20 DAF. An increase in amylose content during early developmental stage has also been reported for the rice (Briones, Magbanua, & Juliano, 1968). Granule bound starch synthase I (GBSSI) is the primary enzyme for amylose biosynthesis in the storage organ. The mRNA of rice GBSSI increases with the development of endosperm (Dian, Jiang, & Wu, 2005). Thus, the increase in GBSSI expression is directly related to the increase in the amylose content of starch during the rice kernel development.

Like that of TQ starches, the amylose contents of TRS starches also increased with the kernel development from 5.4% on 3 DAF to 17.0% on 7 DAF, 37.5% on 10 DAF, 49.2% on 20 DAF and 52.6% on 30 DAF (Fig. 2). This result suggested that the amylose contents had a more rapid increase in TRS than in TQ from 7 DAF to 10 DAF. As expected, the amylose content in TRS was considerably higher than that in TQ. But the amylose contents of TQ and TRS starches did not show marked difference before 7 DAF, especially on 3 DAF. Starch branching enzymes play an essential role in starch biosynthesis by introducing α-1,6-glucosidic linkages into α-1,4-glucosidic chains, and are therefore crucial in determining the structure and physical properties of the synthesized starch. The inactivation of starch branching enzyme IIb in rice is traditionally associated with elevated apparent amylose content (Butardo et al., 2011). In TRS, starch branching enzymes are inhibited through an antisense RNA technique during kernel development (Zhu et al., 2011). So, the amylose contents in TRS starches were significantly higher than that in TQ starches during kernel development.

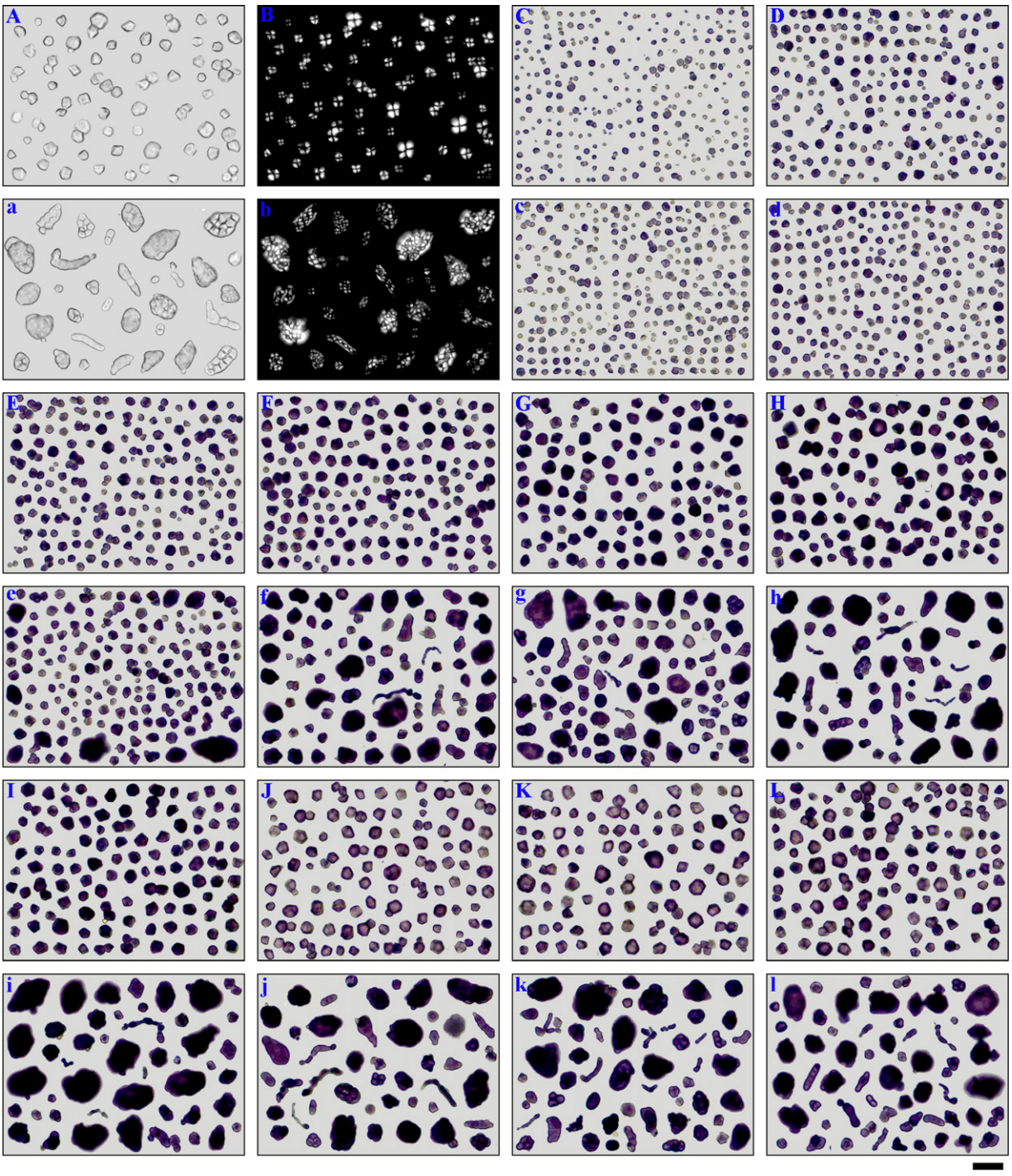


**Fig. 1.** Light micrographs of endosperm starches isolated from TQ and TRS kernels harvested at different developmental stages. (A–L) TQ starches, (a–l) TRS starches. (A, B, a and b) Starches isolated from mature kernels without iodine staining under polarized light microscope for normal light (A and a) and polarized light (B and b). (C–L, c–l) Iodine-stained starches isolated from developing endosperm on 3 DAF (C and c), 5 DAF (D and d), 7 DAF (E and e), 10 DAF (F and f), 13 DAF (G and g), 16 DAF (H and h), 20 DAF (I and i), 25 DAF (J and j), 30 DAF (K and k), and mature kernels (L and l). Scale bar = 10 μm.

### 3.3. XRD spectra of developing starches

The XRD spectra of endosperm starches isolated from TQ and TRS kernels harvested at different developmental stages are shown in Fig. 3. According to XRD pattern, there are three types of starch crystallinity reported, known as A-, B-, and C-type. Usually, the C-type crystallinity is a mixture of both A- and B-type. So, the C-type pattern is classified as $C_A$- (closer to A-type), C-, and $C_B$-type (closer to B-type) according to the proportion of A- and B-allomorph in C-type starch (Cheetham & Tao, 1998). All of TQ starches displayed an A-type crystalline pattern which was characterized by peaks at 15°, 17°, 18° and 23° 2$\theta$ (Fig. 3A). The XRD revealed that the crystalline pattern of TQ starch was not affected by the developmental stages. In other words, the pattern of double helical packing in crystalline lamella of starches from different stages was not different, which was in agreement with previous report (Briones et al., 1968).

TRS starches also displayed a typical A-type crystalline pattern on 3 DAF. The patterns of TRS starches on 5 DAF and 7 DAF were the

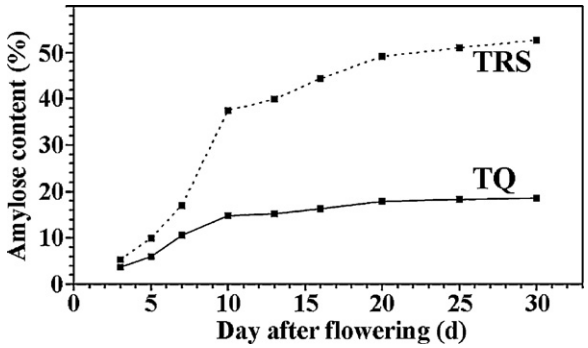


**Fig. 2.** Amylose contents of endosperm starches isolated from TQ and TRS kernels harvested at different developmental stages.

same as A-type crystallinity except for the presence of the medium peak of 5.6° 2$\theta$, which indicated the occurrence of B-type allomorph in starch, and the lower peak of 18° 2$\theta$. Therefore, TRS starches on 5 DAF and 7 DAF showed a $C_A$-type crystallinity. With endosperm development, the intensity of peak gradually increased at 5.6° 2$\theta$ and decreased at 18° 2$\theta$, the peak at 23° 2$\theta$ became broad, and the intensity of peak at 20° 2$\theta$ increased. These were typical characteristics of C-type crystallinity, so TRS starch crystallinity changed from A- to C- via $C_A$-type during kernel development (Fig. 3B). This result is markedly different from high-amylose maize starch, which displays the B-type crystallinity during kernel development (Jiang, Lio et al., 2010). The above results indicated that the development of TRS starches was accompanied by the formation of more B-type crystallinity during kernel development.

The relative crystallinities of TQ and TRS starches decreased (Fig. 3C) with kernel development and the increase in amylose content, which agreed with the previous report that the crystallinity decreases with the increase in amylose content (Cheetham & Tao, 1998). The starches on 3 DAF had the greatest crystallinity, resulting from their larger amylopectin content. The crystallinity in TRS starches was considerably lower than that in TQ starches, which was in agreement with the different amylose contents in TQ and TRS starches (Fig. 2).

### 3.4. ATR-FTIR spectra of developing starches

The development of sampling devices like ATR-FTIR combined with procedures for spectrum deconvolution provides opportunities for the study of starch structure (Sevenou, Hill, Farhat, & Mitchell, 2002). According to the theory of ATR-FTIR, the penetration depth is related to the wavelength. Polysaccharides, like starch, absorb in the region 1200–800 $cm^{-1}$ i.e. at wavelength between ~8 and 12 μm. In this region, the average penetration depth is ~2 μm. Therefore, ATR-FTIR is used to study the external regions of starch granules. Though FTIR is not able to differentiate between A- and B-type crystalline polymorphs, the variation between starch varieties is interpreted in terms of the level of ordered structure present on the edge of starch granules (Sevenou et al., 2002).

The deconvoluted ATR-FTIR spectra in the region 1200–900 $cm^{-1}$ of TQ and TRS developing starches are presented in Fig. 4. TQ starches showed similar ATR-FTIR spectra during kernel development (Fig. 4A). The ATR-FTIR spectra of TRS starches had some changes with kernel development. From 3 to 7 DAF, the spectra in TRS were similar to that in TQ. After 10 DAF, TRS spectra were different from TQ spectra (Fig. 4B). The bands at 1045 and 1022 $cm^{-1}$ are linked with order/crystalline and amorphous regions in starch, respectively. The ratio of absorbance 1045/1022 $cm^{-1}$ is used to quantify the degree of order in starch samples (Sevenou et al., 2002). Intensity ratios of 1045/1022 and 1022/995 $cm^{-1}$ are useful as a convenient index of FTIR

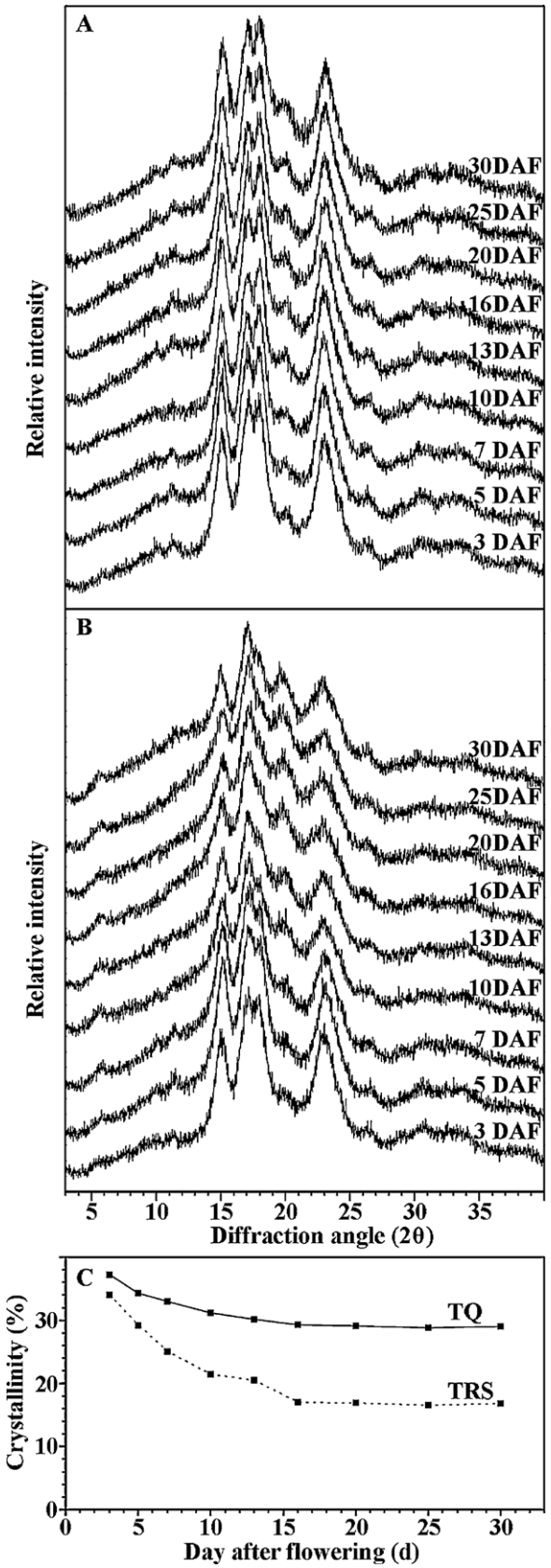


**Fig. 3.** XRD spectra and the crystallinity of endosperm starches isolated from TQ and TRS kernels harvested at different developmental stages. (A) TQ, (B) TRS and (C) Crystallinity at different days after flowering.

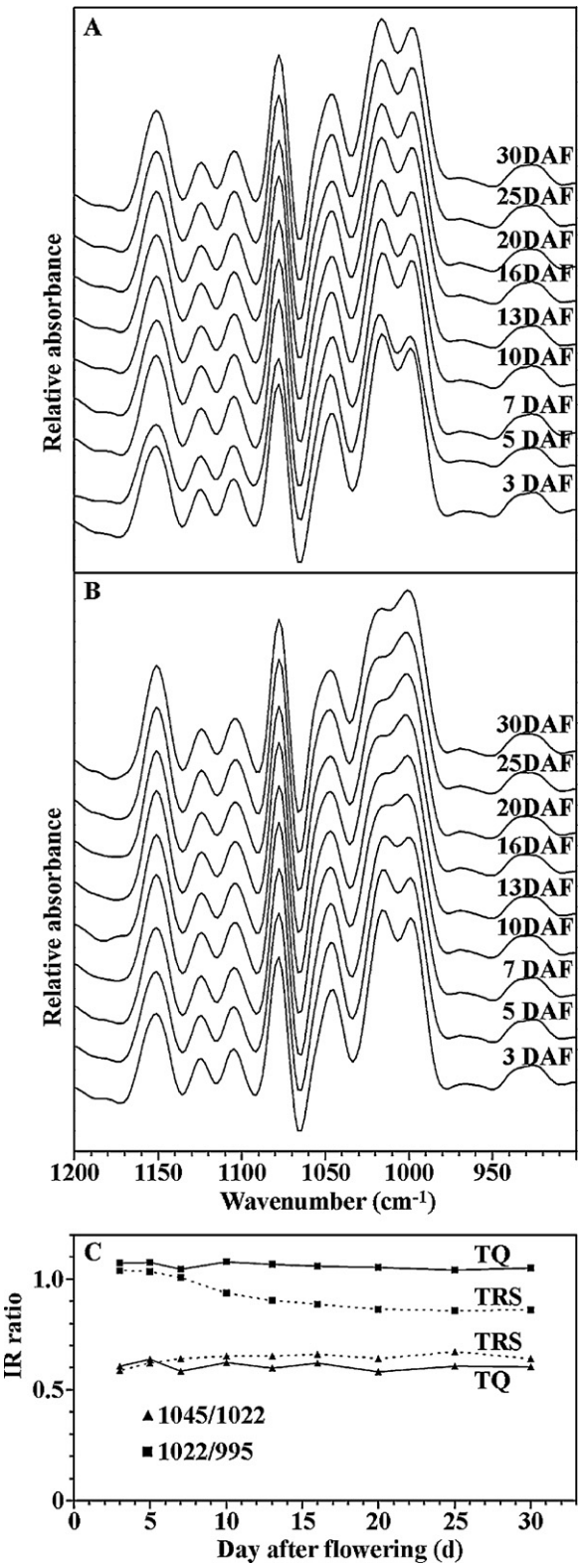


**Fig. 4.** ATR-FTIR deconvoluted spectra and the absorbance ratio of endosperm starches isolated from TQ and TRS kernels harvested at different developmental stages. (A) TQ, (B) TRS, (C) The IR ratio of absorbance at 1045/1022 and 1022/995 $cm^{-1}$.

data in comparisons with other measures of starch conformation (Sevenou et al., 2002). The relative intensities of FTIR bands of TQ and TRS starches at 1045, 1022, and 995 $cm^{-1}$ were recorded from the baseline to peak height, and the ratios for 1045/1022 and 1022/995 $cm^{-1}$ were calculated as shown in Fig. 4C. On the basis of both the spectra and calculated data, the TQ and TRS starches did not show significant differences at early developmental stage (from 3 to 7 DAF). After 7 DAF, the intensity of the band was lower at 1022 $cm^{-1}$ than at 995 $cm^{-1}$ in TRS starch, which was significantly different from TQ starch. A-type waxy maize and normal maize starches show similar intensities of the bands at 1022 and 995 $cm^{-1}$. However, the intensity of the band was significantly lower at 1022 $cm^{-1}$ than at 995 $cm^{-1}$ in B-type amylomaize starch (Sevenou et al., 2002). After 7 DAF, B-type crystallinity was synthesized and deposited in the periphery of TRS starch granules (Fig. 3; Wei, Qin, Zhou et al., 2010), which resulted in the FTIR changes after 7 DAF.

### 3.5. Thermal properties of developing starches

Fig. 5A presents the gelatinization thermograms of endosperm starches isolated from TQ and TRS kernels harvested on 3 and 30 DAF. DSC thermograms of starches from 5 to 25 DAF were similar to that of 3 DAF, or 30 DAF, thus, are not shown. TQ and TRS starches showed one endothermic peak before 20 DAF and 16 DAF respectively. An additional second peak first appeared on 16 DAF in TRS starches and 20 DAF in TQ starches, became a minor peak with kernel development, and then developed into a significant peak on 30 DAF. The intensity of the second peak is significantly higher in TRS starches than that in TQ starches (Fig. 5A). The first peak represents the transition induced by melting of the amylopectin crystallites, and the second peak represents the transition due to dissociation of the amylose-lipid complex (Soulaka & Morrison, 1985). Jiang, Lio et al. (2010) reported that the intensity of second peak coincided with the lipid content of high-amylose maize starch, and the second peak disappeared after removal of lipids from the starch. The lipid contents of starches increased with kernel maturation. They thought that the second peak corresponded to the melting the amorphous amylose–lipid complex (Jiang, Lio et al., 2010).

The thermal properties of TQ and TRS developing starches are summarized in Table 1. A similar gelatinization temperature and enthalpy were observed in TRS and TQ starches on 3 DAF. However, TQ and TRS starches showed significantly different trends of changes of gelatinization properties with kernel development. TQ starches showed a decrease in gelatinization temperature and enthalpy, whereas TRS starches showed an increase in gelatinization temperature and a fast decrease in gelatinization enthalpy (Fig. 5A and Table 1). So, significantly different gelatinization temperature and enthalpy were observed in TRS and TQ starches on 30 DAF. TRS starches showed a significantly higher gelatinization temperature and lower enthalpy compared with TQ starches. These results were consistent with the thermal properties of TRS and TQ starches isolated from the mature kernel (Wei et al., 2011). Gelatinization enthalpy primarily reflects the loss of double helical order and decreases with amylose content increase (Cooke & Gidley, 1992). During kernel development, the decrease of gelatinization enthalpy was consistent with the observation that developing starch had a higher amylose content and lower crystallinity, and required less energy for gelatinization. TRS starch had a significantly higher amylose content and lower crystallinity than TQ starches did at the middle and late developmental stages. So, TRS starches required less energy for gelatinization, and showed a significantly lower gelatinization enthalpy compared with TQ starches. For normal starch, the gelatinization temperature decreases with an increase in amylose content. But for high-amylose starch, the B-type crystalline form of amylopectin

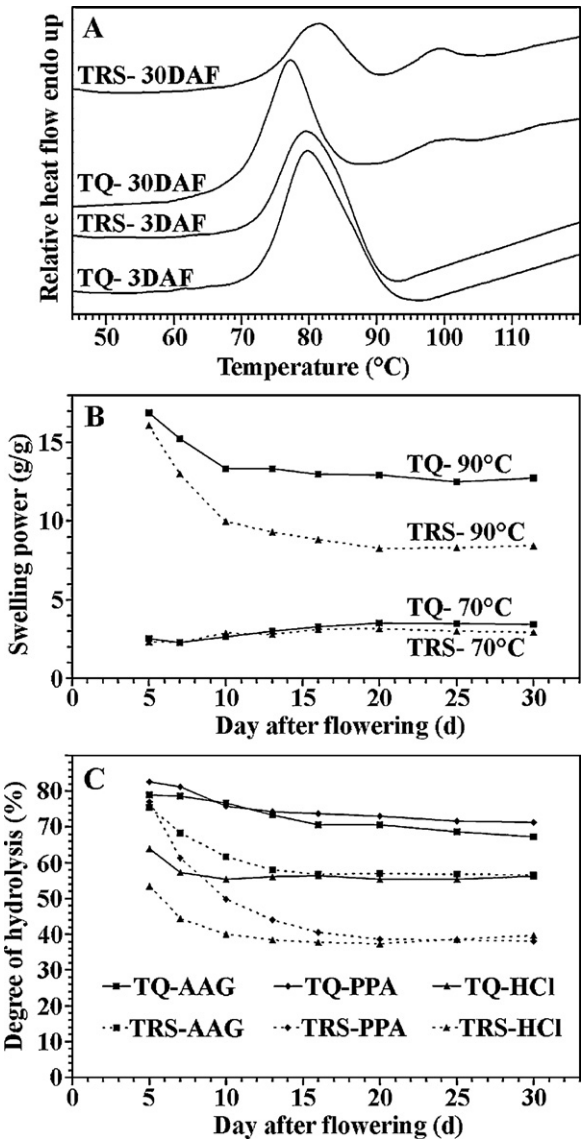


**Fig. 5.** Representative DSC thermograms (A), swelling powers (B) and hydrolysis rates (C) of TQ and TRS developing starches.

results in higher gelatinization temperature than normal starch (Richardson, Jeffcoat, & Shi, 2000), amylose double helices also require high temperature and energy to disorder and therefore lead to a high gelatinization temperature (Shi, Capitani, Trzasko, & Jeffcoat, 1998). Amylose content significantly increased, and B-type allomorph formed in TRS endosperm starches at middle and late developmental stages, which resulted in the increase of gelatinization temperature in TRS starches.

### 3.6. Swelling powers of developing starches

According to starch gelatinization temperature (Table 1), we investigated the swelling powers of TQ and TRS developing starches at 70 °C (before gelatinization) and 90 °C (after gelatinization) (Fig. 5B). Before gelatinization, swelling powers slightly increased with kernel development before 20 DAF, whereas no difference was observed between TQ and TRS starches. After gelatinization, swelling power decreased with kernal development. At early developmental stage (on 5 DAF), TRS and TQ had similar swelling powers. After 10 DAF, TRS starches had significantly lower swelling powers than TQ did, which was in agreement with TRS and TQ starches isolated from mature kernels (Wei et al., 2011). The high-amylose rice mutant has also a much lower swelling power compared with that of its wild type rice (Kang et al., 2003). Swelling power tests are simple analyses that measure the uptake of water during the gelatinization of starch. Amylopectin is considered to contribute to water absorption, swelling and pasting of starch granules, whereas amylose and lipids tend to retard these processes (Tester & Morrison, 1990). The linear amylose diffuses out of the swollen granules and makes up the continuous phase outside the granules as a restraint to swelling. So, an inverse correlation was found between amylose content and swelling power (Hermansson & Svegmark, 1996).

### 3.7. Hydrolysis properties of developing starches

Developing starches from TQ and TRS were subjected to 1 day of hydrolysis by PPA and AAG, and 4 days of hydrolysis by HCl (Fig. 5C). The hydrolysis rates of TQ starches slowly decreased with kernel development from 82.7% on 5 DAF to 71.3% on 30 DAF for PPA, from 78.9% on 5 DAF to 67.3% on 30 DAF for AAG, and from 63.9% on 5 DAF to 56.2% on 30 DAF for HCl. By contrast, the hydrolysis rates of TRS starches decreased rapidly with kernel development from 77.1% on 5 DAF to 38.0% on 30 DAF for PPA, from 75.5% on 5 DAF to 56.7% on 30 DAF for AAG, and from 53.4% on 5 DAF to 39.6% on 30 DAF for HCl. The fast decrease of hydrolysis rate of TRS

**Table 1**
Thermal properties of endosperm starches isolated from TQ and TRS kernels harvested at different developmental stages.

| Starch | TQ | | | | TRS | | | |
|---|---|---|---|---|---|---|---|---|
| | $T_o$ (°C)[a] | $T_p$ (°C)[a] | $T_c$ (°C)[a] | $\Delta H$ (J/g)[a] | $T_o$ (°C)[a] | $T_p$ (°C)[a] | $T_c$ (°C)[a] | $\Delta H$ (J/g)[a] |
| 3 DAF | 72.5 | 79.7 | 91.6 | 21.6 | 71.3 | 79.6 | 89.9 | 21.0 |
| 5 DAF | 74.3 | 79.2 | 86.7 | 19.3 | 72.9 | 80.6 | 88.7 | 16.9 |
| 7 DAF | 74.0 | 80.1 | 87.3 | 16.5 | 72.7 | 82.0 | 89.8 | 18.4 |
| 10 DAF | 74.3 | 79.2 | 85.8 | 15.7 | 72.3 | 81.8 | 88.9 | 15.5 |
| 13 DAF | 72.2 | 78.4 | 84.8 | 14.9 | 73.3 | 81.8 | 89.8 | 13.5 |
| 16 DAF | 72.5 | 77.8 | 84.0 | 13.1 | 72.0 | 80.2 | 89.2 | 11.8 |
| 16 DAF[b] | nd[c] | nd[c] | nd[c] | nd[c] | 95.1 | 100.8 | 105.6 | 0.5 |
| 20 DAF | 72.8 | 78.1 | 84.0 | 12.9 | 72.9 | 80.0 | 89.3 | 10.6 |
| 20 DAF[b] | 94.3 | 97.8 | 103.6 | 0.3 | 93.6 | 100.0 | 106.4 | 1.1 |
| 25 DAF | 72.4 | 78.1 | 83.8 | 12.5 | 72.7 | 81.0 | 89.8 | 9.2 |
| 25 DAF[b] | 92.1 | 98.4 | 103.1 | 0.6 | 93.4 | 99.7 | 107.5 | 1.4 |
| 30 DAF | 69.3 | 77.2 | 84.4 | 12.5 | 73.4 | 81.7 | 89.0 | 7.6 |
| 30 DAF[b] | 92.3 | 101.2 | 104.8 | 0.8 | 93.4 | 99.4 | 104.3 | 1.6 |

[a] $T_o$, onset temperature; $T_p$, peak temperature; $T_c$, conclusion temperature; ΔH, gelatinization enthalpy.
[b] Thermal parameters of the second peak.
[c] nd, not detectable.

starches occurred before 20 DAF, especially from 5 to 10 DAF. TQ and TRS starches on 5 DAF had similar hydrolysis rate by PPA and AAG, but TRS starches had higher resistance to enzyme digestion and acid hydrolysis than TQ starches did with kernel development (Fig. 5C). TRS starches isolated from mature kernels also show a higher resistance to *Bacillus species* α-amylase digestion and acid hydrolysis than TQ starches do (Wei, Xu et al., 2010).

α-Amylase is an endo-amylase that catalyses the hydrolysis of internal α-1,4-glycosidic linkages in starch in a random manner. Glucoamylase is an exo-amylase that cleaves D-glucose from the nonreducing ends of starch. Susceptibility of starch to enzyme attack is influenced by factors such as amylose to amylopectin ratio, crystalline structure, particle size and relative surface area, granule integrity, porosity of granules, and structural heterogeneities (Blazek & Copeland, 2010). The A-, B- and C-type starches show different susceptibilities to α-amylase hydrolysis. Generally, A-type starches are more readily hydrolyzed by α-amylase than B- or C-type starches (You & Izydorczyk, 2007). It is reported that the amount of native starch hydrolysis by amylase or acid is inversely related to the amylose content (Li, Vasanthan, Rossnagel, and Hoover, 2001; Li et al., 2004). TQ starches are organized as compound starches and dissociated to separate individual starch subgranules during starch isolation. Whereas TRS starches are organized as semicompound starches with a thick continuous band encircling the entire circumference of starch subgranules. These subgranules are not dissociated during starch isolation, therefore, the sizes of isolated TRS starch granules are larger than that of TQ starch subgranule, and the relative surface area of TRS starches is smaller than that of TQ starches (Wei, Qin, Zhu et al., 2010). TRS starch is compound starch before 6 DAF, then gradually becomes semicompound starch from 6 to 10 DAF. During this stage, the amylose content increases, and the B-type allomorph is synthesized and deposited in the periphery of TRS starch subgranules (Wei, Qin, Zhou et al., 2010). Therefore, we thought that the decrease in the relative surface area, the increase in amylose content, and the B-type allomorph deposition of TRS starches resulted in higher resistance to enzyme digestion and acid hydrolysis.

### 3.8. Correlation analysis between amylose content and physicochemical properties of developing starches

Fig. 6 shows plots of amylose content vs. some physicochemical properties. The regression lines were made in order to compare the correlation between amylose content and physicochemical properties. The amylose content had a highly significantly negative correlation with crystallinity, gelatinization enthalpy, swelling power at 90 °C, and hydrolysis rate by AAG, PPA, and HCl. The correlation coefficients were −0.97, −0.82, −0.97, −0.96, −0.98, and −0.92, respectively ($P < 0.001$) (Fig. 6). Amylose content is the major factor controlling almost all physicochemical properties of rice starch (Wickramasinghe & Noda, 2008). Cheetham and Tao (1998) reported that amylose content had a significantly negative correlation with crystallinity. Wickramasinghe and Noda (2008) analyzed amylose content, swelling power, pasting properties by Rapid Visco Analyzer, thermal properties by DSC, and enzymatic digestibility of starches isolated from 19 different Sri Lankan rice varieties. Their results showed that amylose content correlated negatively to the peak and breakdown viscosities and enzyme digestibility, but positively to the swelling power and enthalpy. Fredriksson, Silverio, Andersson, Eliasson, and Åman (1998) suggested that amylose restrained the swelling of starch, and decreased gelatinization enthalpy. Our results suggested that amylose content played a significant role in reducing crystallinity, gelatinization enthalpy, swelling power, enzyme digestibility, and acid hydrolysis.

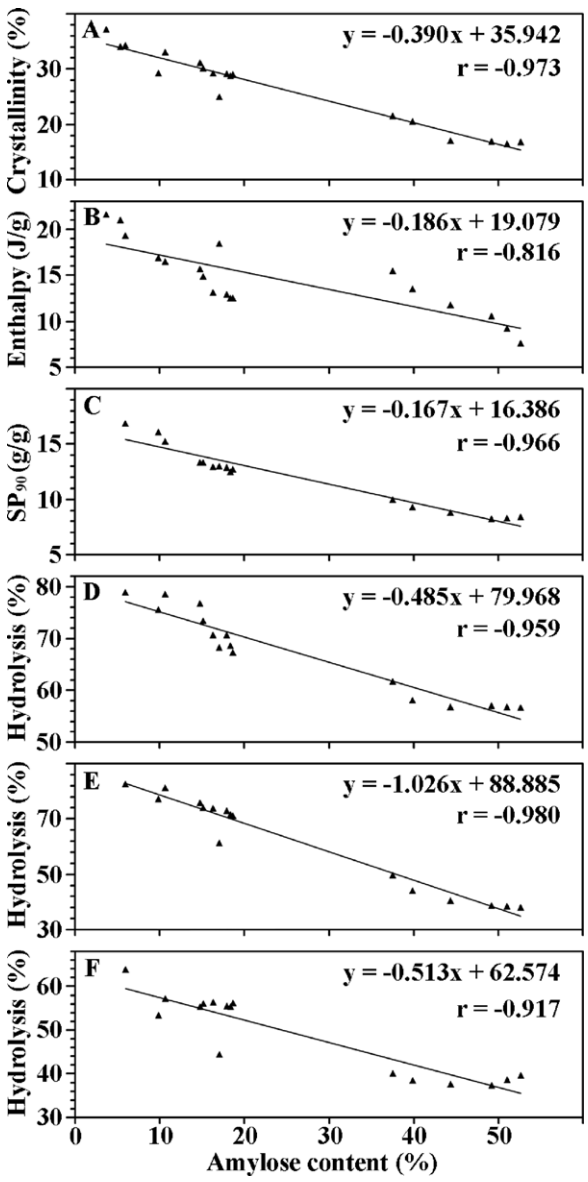


**Fig. 6.** The correlation between amylose content and crystallinity (A), gelatinization enthalpy (B), swelling power at 90 °C ($SP_{90}$) (C), hydrolysis rate by AAG (D), hydrolysis rate by PPA (E), and hydrolysis rate by HCl (F). $P < 0.001$ for (A)–(F).

## 4. Conclusion

In conclusion, endosperm starches were isolated from TQ and TRS kernels harvested at different developmental stages. TQ and TRS starches showed similar amylose contents and shapes on 3 DAF, then the amylose content increased with kernel development. The rate of increase in amylose content was extremely faster in TRS starches than that in TQ starches at early and middle developmental stages, which resulted in significantly different physicochemical properties between TQ and TRS starches after 10 DAF. TRS starches showed heterogeneous granules after 10 DAF. TQ starch crystallinity remained A-type, but TRS starch crystallinity changed from A- to C- via $C_A$-type. TRS starches had lower crystallinity than TQ starches did. TRS starches showed higher gelatinization temperature and lower gelatinization enthalpy at middle and late developmental stages compared with TQ starches. However, no significant difference in gelatinization temperature and enthalpy was observed in TQ and TRS starches on 3 DAF. TRS and TQ starch had similar swelling power and hydrolysis rate on 5 DAF,

but TRS starches showed lower swelling power and hydrolysis rate by AAG, PPA, and HCl after 10 DAF. The amylose content had a significantly negative correlation with crystallinity, gelatinization enthalpy, swelling power, enzyme digestibility, and acid hydrolysis. These results would be very useful for the understanding of the formation and structure of starch granule during kernel development and for breeding of high-amylose cereal crops.

## Acknowledgements

This study was financially supported by grants from the Ministry of Science and Technology of China (2012CB944803), the National Natural Science Foundation of China (31071342), and the Government of Jiangsu Province (the Priority Academic Program Development of Jiangsu Higher Education Institutions, BK2009186).

## References

Blazek, J., & Copeland, L. (2010). Amylolysis of wheat starches II. Degradation patterns of native starch granules with varying functional properties. *Journal of Cereal Science*, *52*, 295–302.

Briones, V. P., Magbanua, L. G., & Juliano, B. O. (1968). Changes in physicochemical properties of starch of developing rice grain. *Cereal Chemistry*, *45*, 351–357.

Butardo, V. M., Fitzgerald, M. A., Bird, A. R., Gidley, M. J., Flanagan, B. M., Larroque, O., Resurreccion, A. P., Laidlaw, H. K. C., Jobling, S. A., Morell, M. K., & Rahman, S. (2011). Impact of down-regulation of starch branching enzyme IIb in rice by artificial microRNA- and hairpin RNA-mediated RNA silencing. *Journal of Experimental Botany*, *62*, 4927–4941.

Cheetham, N. W. H., & Tao, L. (1998). Variation in crystalline type with amylose content in maize starch granules: An X-ray powder diffraction study. *Carbohydrate Polymers*, *36*, 277–284.

Cooke, D., & Gidley, M. J. (1992). Loss of crystalline and molecular order during starch gelatinization: Origin of the enthalpic transition. *Carbohydrate Research*, *227*, 103–112.

Dian, W., Jiang, H., & Wu, P. (2005). Evolution and expression analysis of starch synthase III and IV in rice. *Journal of Experimental Botany*, *56*, 623–632.

Englyst, H. N., Kingman, S. M., & Cummings, J. H. (1992). Classification and measurement of nutritionally important starch fractions. *European Journal of Clinical Nutrition*, *46*, S33–S50.

Fredriksson, H., Silverio, J., Andersson, R., Eliasson, A. C., & Åman, P. (1998). The influence of amylose and amylopectin characteristics on gelatinization and retrogradation properties of different starches. *Carbohydrate Polymers*, *35*, 119–134.

Hermansson, A. M., & Svegmark, K. (1996). Developments in the understanding of starch functionality. *Trends in Food Science and Technology*, *7*, 345–353.

Jiang, H. X., Campbell, M., Blanco, M., & Jane, J. L. (2010). Characterization of maize amylose-extender (*ae*) mutant starches Part II: Structures and properties of starch residues remaining after enzyme hydrolysis at boiling-water temperature. *Carbohydrate Polymers*, *80*, 1–12.

Jiang, H. X., Horner, H. T., Pepper, T. M., Blanco, M., Campbell, M., & Jane, J. L. (2010). Formation of elongated starch granules in high-amylose maize. *Carbohydrate Polymers*, *80*, 533–538.

Jiang, H. X., Lio, J. Y., Blanco, M., Campbell, M., & Jane, J. L. (2010). Resistant-starch formation in high-amylose maize starch during kernel development. *Journal of Agricultural and Food Chemistry*, *58*, 8043–8047.

Kang, H. J., Hwang, I. K., Kim, K. S., & Choi, H. C. (2003). Comparative structure and physicochemical properties of Ilpumbyeo, a high-quality japonica rice, and its mutant, Suweon 464. *Journal of Agricultural and Food Chemistry*, *51*, 6598–6603.

Li, J. H., Vasanthan, T., Hoover, R., & Rossnagel, B. G. (2004). Starch from hull-less barley. V. In vitro susceptibility of waxy, normal, and high-amylose starches towards hydrolysis by alpha-amylases and amyloglucosidase. *Food Chemistry*, *84*, 621–632.

Li, J. H., Vasanthan, T., Rossnagel, B., & Hoover, R. (2001). Starch from hullless barley. II. Thermal, rheological and acid hydrolysis characteristics. *Food Chemistry*, *74*, 407–415.

Nugent, A. P. (2005). Health properties of resistant starch. *Nutrition Bulletin*, *30*, 27–54.

Regina, A., Bird, A., Topping, D., Bowden, S., Freeman, J., Barsby, T., Kosar-Hashemi, B., Li, Z. Y., Rahman, S., & Morell, M. (2006). High-amylose wheat generated by RNA interference improves indices of large-bowel health in rats. *Proceedings of the National Academy of Sciences of USA*, *103*, 3546–3551.

Richardson, P. H., Jeffcoat, R., & Shi, Y. C. (2000). High-amylose starches: From biosynthesis to their use as food ingredients. *MRS Bulletin*, *25*(12), 20–24.

Sang, Y. J., Bean, S., Seib, P. A., Pedersen, J., & Shi, Y. C. (2008). Structure and functional properties of sorghum starches differing in amylose content. *Journal of Agricultural and Food Chemistry*, *56*, 6680–6685.

Sevenou, O., Hill, S. E., Farhat, I. A., & Mitchell, J. R. (2002). Organisation of the external region of the starch granule as determined by infrared spectroscopy. *International Journal of Biological Macromolecules*, *31*, 79–85.

Shannon, J. C., & Garwood, D. L. (1984). Genetics and physiology of starch development. In R. L. Whistler, J. N. Bemiller, & E. F. Paschall (Eds.), *Starch: Chemistry and Technology* (pp. 25–86). New York: Academic Press.

Shi, Y. C., Capitani, T., Trzasko, P., & Jeffcoat, R. (1998). Molecular structure of a low-amylopectin starch and other high-amylose maize starches. *Journal of Cereal Science*, *27*, 289–299.

Soulaka, A. B., & Morrison, W. R. (1985). The amylose and lipid contents, dimensions, and gelatinsation characteristics of some wheat starches and their A-and B-granule fractions. *Journal of the Science of Food and Agriculture*, *36*, 709–718.

Tester, R. F., & Morrison, W. R. (1990). Swelling and gelatinisation of cereal starches. I. Effects of amylopectin, amylose and lipids. *Cereal Chemistry*, *67*, 551–557.

Viles, F. J., Jr., & Silverman, L. (1949). Determination of starch and cellulose with anthrone. *Analytical Chemistry*, *21*, 950–953.

Wei, C. X., Qin, F. L., Zhou, W. D., Chen, Y. F., Xu, B., Wang, Y. P., Gu, M. H., & Liu, Q. Q. (2010). Formation of semi-compound C-type starch granule in high-amylose rice developed by antisense RNA inhibition of starch-branching enzyme. *Journal of Agricultural and Food Chemistry*, *58*, 11097–11104.

Wei, C. X., Qin, F. L., Zhou, W. D., Xu, B., Chen, C., Chen, Y. F., Wang, Y. P., Gu, M. H., & Liu, Q. Q. (2011). Comparison of the crystalline properties and structural changes of starches from high-amylose transgenic rice and its wild type during heating. *Food Chemistry*, *128*, 645–652.

Wei, C. X., Qin, F. L., Zhu, L. J., Zhou, W. D., Chen, Y. F., Wang, Y. P., Gu, M. H., & Liu, Q. Q. (2010). Microstructure and ultrastructure of high-amylose rice resistant starch granules modified by antisense RNA inhibition of starch branching enzyme. *Journal of Agricultural and Food Chemistry*, *58*, 1224–1232.

Wei, C. X., Xu, B., Qin, F. L., Yu, H. G., Chen, C., Meng, X. L., Zhu, L. J., Wang, Y. P., Gu, M. H., & Liu, Q. Q. (2010). C-type starch from high-amylose rice resistant starch granules modified by antisense RNA inhibition of starch branching enzyme. *Journal of Agricultural and Food Chemistry*, *58*, 7383–7388.

Wickramasinghe, H. A. M., & Noda, T. (2008). Physicochemical properties of starches from Sri Lankan rice varieties. *Food Science and Technology Research*, *14*, 49–54.

You, S., & Izydorczyk, M. S. (2007). Comparison of the physicochemical properties of barley starches after partial α-amylolysis and acid/alcohol hydrolysis. *Carbohydrate Polymers*, *69*, 489–502.

Zhu, L. J., Gu, M. H., Meng, X. L., Cheung, S. C. K., Yu, H. X., Huang, J., Sun, Y., Shi, Y. C., & Liu, Q. Q. (2011). High-amylose rice improves indices of animal health in normal and diabetic rats. *Plant Biotechnology Journal*, doi:10.1111/j.1467-7652.2011.00667.x